IOP PUBLISHING JOURNAL OF PHYSICS: CONDENSED MATTER

J. Phys.: Condens. Matter **19** (2007) 455206 (10pp) doi:10.1088/0953-8984/19/45/455206

An intermediate phase in Ge_xSe_{1-x} glasses: experiment and simulation

F Inam[1], M T Shatnawi[2], D Tafen[3], S J L Billinge[2], Ping Chen[4] and D A Drabold[1]

[1] Department of Physics and Astronomy, Ohio University, Athens, OH 45701, USA
[2] Department of Physics and Astronomy, Michigan State University, East Lansing, MI 48824-1116, USA
[3] Physics Department, West Virginia University, Morgantown, WV 26506, USA
[4] Department of ECECS, University of Cincinnati, Cincinnati, OH 45221, USA

Received 31 July 2007
Published 24 October 2007
Online at stacks.iop.org/JPhysCM/19/455206

Abstract

The pair correlation function for Ge_xSe_{1-x} alloys near the intermediate phase (IP) is reported. First-principles MD models of these alloys show a 'self-organized' phase associated with the number of Ge bonds with twofold Se atoms. This probably represents the IP of Boolchand. The self-organization involves maintaining a nearly constant number of twofold Se atoms bonded to *one* Ge atom through a range of Ge concentration, roughly coinciding with the IP. This behavior is manifested in observables like the optical gap. Our work suggests that the IP is due to selective formation of these local structures.

(Some figures in this article are in colour only in the electronic version)

1. Introduction

A good deal of work has been done on the network properties (intermediate range order (IRO), rigidity transitions etc) of Ge_xSe_{1-x} glasses which change considerably with the concentration x of Ge. IRO (attributed to the first sharp diffraction peak (FSDP) in the static structure factor of these alloys) is reported to increase with the concentration of Ge [1]. A floppy to rigid network transition was predicted for a covalent bond network [2, 3] and is observed from Raman and high pressure Raman experiments on these alloys. The transition occurs through an extended composition range $x \in (0.20, 0.25)$, the intermediate phase (IP) [4–6]. The IP is also observed in other binary chalcogenide materials like Si_xSe_{1-x} [7]. The IP picture was first developed by Thorpe *et al* [8] by proposing that an unstressed rigid intermediate phase may arise when system self-organizes to minimize the stress. Micoulaut and Phillips [9, 10] approached the problem by constructing networks of binary chalcogenide glasses with a size increasing cluster approximation (SICA) showing that the floppy to rigid transition through an unstressed intermediate phase can be obtained by cluster construction and constraint counting. Other approaches to the IP have been proposed by a number of authors [11].

There was a suggestion of a structural response to the IP in data of Sharma *et al* [12], but this result has not been reproduced in recent measurements on the samples used in this study [13].

Here we report x-ray diffraction (XRD) measurements on Ge_xSe_{1-x} alloys and discuss models of these alloys obtained from first-principles MD simulations. Analysis of the topology of these models suggests that self-organization is associated with the population of specific local bonding units, and the evolution of these units with Ge concentration x. In particular, the network maintains a relatively high concentration of isostatic twofold Se units having one Se neighbor and one Ge neighbor through the IP window. We have not computed the vibrational properties of the networks (for example the evolution of the tetrahedral breathing mode frequency as a function of x) to prove the presence of the IP in our models. However the models do exhibit a telltale 'flattening' of network properties in the IP window that strongly suggests the IP discovered experimentally by Boolchand.

2. Experimental details

The starting ingredients (99.9999% Ge and Se) were vacuum sealed (5×10^{-7} Torr) in quartz tubes, heated to 950 °C for four days or more, and thereafter the melt temperatures were slowly lowered to 50 °C above the liquidus. Samples were allowed to age for three weeks before the quartz tubes were opened, and glass transitions examined in modulated-differential scanning calorimetric measurements. A scan rate of 3 °C min^{-1} and a modulation rate of 1 °C/100 s was used to record scans. The samples studied were carefully characterized using T_g, and reverse heat flow and Raman spectroscopy to locate the intermediate phase in this set of samples. The same glasses were then gently crushed into fine powder, formed into disks 5 mm in diameter and 1 mm thick, sealed between thin Kapton foils and subjected to x-ray diffraction experiments. This approach ensured that the samples in the beam were of uniform geometry[5].

The XRD measurements were carried out using the rapid acquisition PDF (RAPDF) technique [14] at the MUCAT 6-ID-D beam line at the advanced photon source (APS), Argonne National Laboratory, at room temperature. The sample–detector distance was calibrated using a silicon standard of known lattice parameter. A representative plot of the two-dimensional XRD pattern collected by MAR345 image plate detector together with the integrated one-dimensional pattern are shown in figure 1. Integration of MAR images was performed using the program Fit2D [15]. Data reduction to obtain the structure functions, $S(Q)$, and the PDF, $G(r)$, were performed using the program PDFgetX2 [16].

3. Computer model preparation

We have used the approximate *ab initio* density functional code FIREBALL developed by Sankey and co-workers [17]. The method has been used very successfully for a variety of covalently bonded systems, and especially glassy germanium selenides [18–20].

We generated a sequence of 500-atom Ge_xSe_{1-x} models with Ge concentrations (x = 0.15, 0.18, 0.22, 0.23, 0.25) using a quench from melt technique. Atoms were randomly placed in a cubic cell with suitable (fixed) volume. The cells were then heated to 4200 K, and then equilibrated at 1500 K for about 3.5 ps. Then, they were quenched to 400 K over about 4.5 ps, using velocity rescaling. Finally, the cells were steepest descent quenched to 0 K. Beside this series we have used models we have proposed earlier like $GeSe_4$ (x = 0.20) and $GeSe_9$

[5] We thank P Boolchand for providing this information on sample preparation.

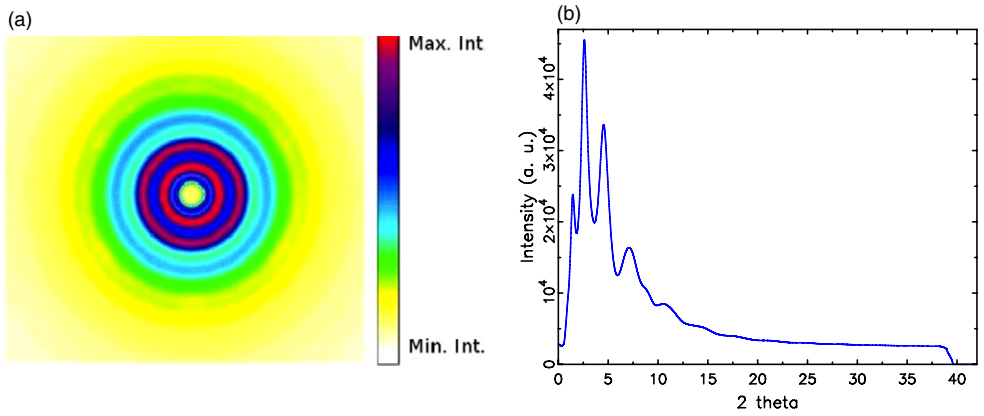

Figure 1. (a) A representative two-dimensional XRD pattern for glassy $Ge_{20}Se_{80}$ sample collected with the MAR345 image plate detector and (b) the integrated one-dimensional XRD pattern.

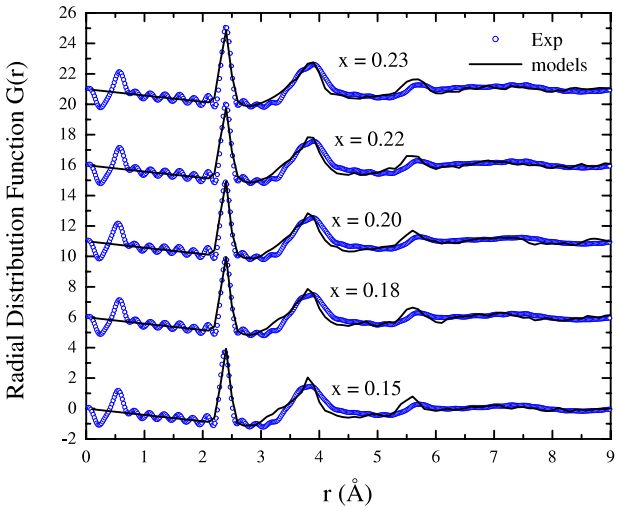

Figure 2. Total radial distribution functions, experiment and theory.

($x = 0.10$) [18] and $GeSe_2$ ($x = 0.33$) by Cobb [19]. All these models have similar densities. Figure 2 shows a qualitative agreement between the total radial distribution functions (RDF) $G(r)$ obtained from the models and experiment. First shells of all models are nicely matched with those of the experiment. Though the peaks of second shells track the experiment, the widths are not perfectly reproduced.

While the agreement between the models and the experimental samples is reasonable, we will use our experimentally constrained molecular relaxation technique [21] in subsequent work to tune the structure of these glasses by using the XRD data as a constraint in the model formation process. The starting point for these calculations will of course be the set of models that we report here. Note that structural changes in $G(r)$ are essentially undetectable through the IP window.

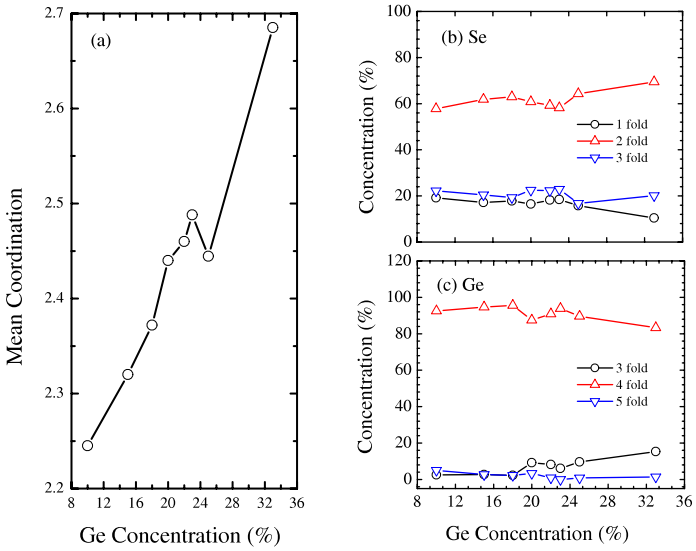

Figure 3. (a) Variation in the mean coordination $\overline{r}$ with Ge content. (b) The change in concentration of onefold, twofold and threefold Se. (c) Concentration of threefold, fourfold and fivefold Ge atoms.

4. Coordination, rings and constraints

In the Ge_xSe_{1-x} system, tetravalent (fourfold) Ge and divalent (twofold) Se are the fundamental building blocks for the network. For x small enough, twofold Se exist in the form of long chains while fourfold tetrahedral Ge connect these chains to each other and form closed rings.

Adding Ge atoms in a Se rich environment increases the mean coordination per atom. The mean coordination $\overline{r}$ is defined as $\frac{\sum_r rn_r}{\sum_r n_r}$, where r runs over all the coordinations present in the system, and n_r is the number of atoms with coordination r. Mean coordination $\overline{r}$ is an important parameter for describing the network. Figure 3(a) shows the increase in $\overline{r}$ with Ge concentration. It is interesting to note that the increase is not linear. Between $x = 0.20$ and 0.25, $\overline{r}$ briefly saturates, suggesting a kind of 'resistance' that the system offers to further increase in the number of bonds per atom. As described later, the signature of this behavior is present in the overall evolution of the network. Figures 3(b) and (c) show the variation in the coordination of the species with Ge concentration. From $x = 0.10$ to 0.18 the concentration of twofold Se increases linearly from 58 to 63%. Between $x = 0.18$ and 0.25 the concentration first decreases, and then abruptly increases to 72%. With increasing Ge concentration, the system gradually eliminates homopolar Se bonds and forms chemically preferred Se–Ge bonds. A consequence is the transition which occurs in the neighbors of twofold Se (figure 4(b)), that is, a gradual replacement of Se neighbors with Ge neighbors. At lower Ge content twofold Se have more Se neighbors than Ge neighbors. Increase in Ge content starts to replace Se with Ge atoms as the neighbors of twofold Se. At $x = 0.20$, the concentration of twofold Se with neighbors Se_1Ge_1 assumes a higher value compared to that for twofold Se with Se_2Ge_0 and Se_0Ge_2 neighbors as shown in figure 4(b). The increase in Se_1Ge_1 units at $x = 0.20$ affects the evolution of corner-sharing tetrahedra (CST) and the ring structure as shown in figure 5. Due to the high concentration of Se_1Ge_1 units in the range $x = 0.2, 0.25$, the concentration of CST and total number of rings tend to saturate in this range (figures 5(a), (b)). It is clear that the transition from all Se neighbors around Se sites to Ge neighbors occurs roughly through

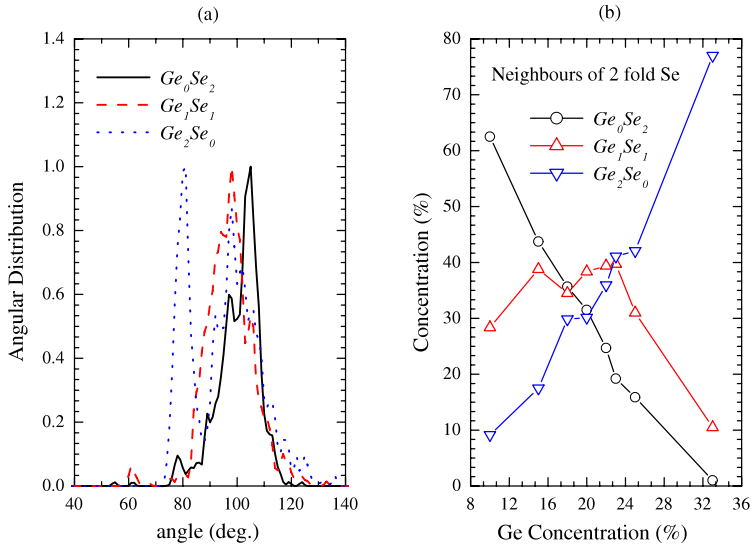

Figure 4. (a) Bond angle distribution of twofold Se units. (b) Variation of concentration of types of neighbors, Se_2Ge_0, Se_1Ge_1 and Se_0Ge_2. Lines are a guide to the eye. Note the 'flattening' of Se_1Ge_1 concentration near the IP window.

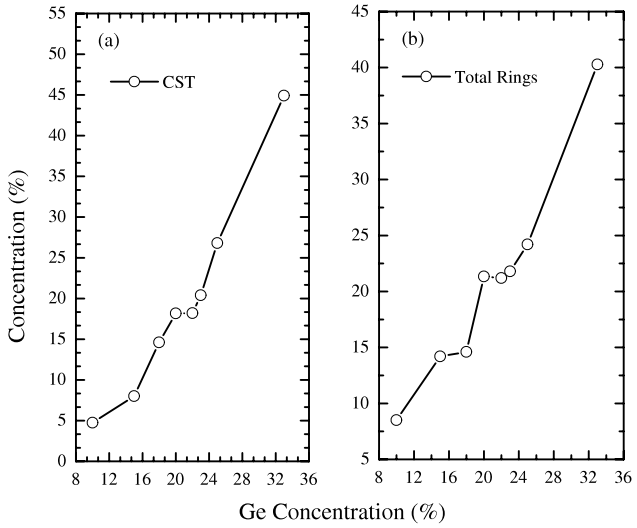

Figure 5. (a) and (b): the concentration of corner-sharing tetrahedra and the total number of rings, respectively.

a range $x \in (0.20, 0.25)$ in which system may be said to 'self-organize'. Below $x = 0.18$, fourfold tetrahedral units reveal a slight increase while there is fluctuation between $x = 0.20$ and 0.25. At $x = 0.20$, threefold Ge increases to a considerable concentration of 10% of Ge content (figure 3(c)).

Figure 4(a) shows the angle distribution for twofold Se units averaged over all x. An interesting feature is the lower angle peak (around 80°) for Se_0Ge_2 units which is due to the formation of fourfold rings (edge-sharing tetrahedra units). Se_1Ge_1 shows a broad shoulder

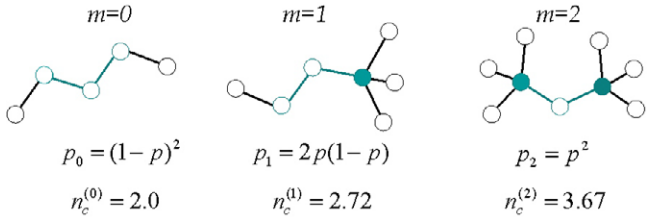

Figure 6. Schematic representation of the formation of twofold Se m units. Open circles represent Se atoms while filled circles are Ge atoms.

around 90° of the main peak centered at about 97°. This shoulder also comes from fourfold rings constituted mainly of one Ge and three Se atoms. Se_2Ge_0 units shows a high peak around 105° due to open chain like structures or larger size rings consisting of mainly Se atoms.

On each of the twofold Se units we can count the number of Lagrangian constraints n_c by adding bond bending and bond stretching constraints. For a $(Ge_{m/r_{Ge}}Se_{(2-m)/r_{Se}})Se$ formula unit (where r_{Ge} and r_{Se} are the coordinations of neighboring Ge and Se atoms and $m = 0, 1, 2$ are the numbers of Ge atoms in the neighbors), constraints are calculated as follows. For each atom of coordination r there are $r/2$ bond stretching and $2r - 3$ bond bending constraints [22]. For $r = 1$ there is only one (bond stretching) constraint [23, 24]. For $r_{Ge} = 4$ and $r_{Se} = 2$, the constraint counts for $m = 0, 1, 2$ are 2.0, 2.72 and 3.67 respectively (figure 6), showing that $m = 0$ and 2 units are underconstrained and rigid respectively, while $m = 1$ units are close to what is called isostatic. If we allow threefold coordination for both Se and Ge neighbors of $m = 1$ units, the constraint count for these units assumes the value 3.0 making them completely isostatic. Since the system does keep a considerable amount of threefold Se and threefold Ge concentration especially in the IP window (figure 3), the constraint count for these units changes. We calculated the constraint counts for each unit for all x. Interestingly, we found that $m = 1$ units assume the value 3.0 in the IP window and this slightly decreases for higher concentration and increases a little for lower concentration. In the IP window, increase in threefold Se and threefold Ge content increases the probability of $m = 1$ units with threefold Se and Ge neighbors; thus most $m = 1$ units become isostatic in the IP window. Total constraint counts n_c for twofold Se units can be calculated as $\sum_m n_c^{(m)} p_m$, where $n_c^{(m)}$ is the constraint count of unit m and p_m is the corresponding concentration of that unit (figure 8). Figure 7 shows a sharp increase in n_c after $x = 0.25$, while it stays close to 3.0 below this Ge composition.

5. Network evolution

Micoulaut and Phillips [10, 9] have modeled the self-organized phase by building the network using a size increasing cluster approximation (SICA). They showed that the network obtained with this approximation can minimize the free energy related to the elastic deformation of the network, in the vicinity of IP window for certain fractions of edge-sharing (ES) tetrahedra, thus making the appearance of a self-organized phase plausible. SICA is a simple and efficient way to construct binary networks which contain ring structures, for example B_2O_3 [25]. The basic idea is to construct the network by joining structures in different possible configurations with corresponding probabilities suited to a given composition. In the case of the Ge_xSe_{1-x} network, basic short range units are Se_2 chain fragments and stoichiometric $GeSe_{4/2}$ molecules. Their corresponding probabilities are given as $1 - p$ and $p = 2x/(1 - x)$ [10] respectively. As described above, the evolution of the network with Ge concentration is mainly driven by

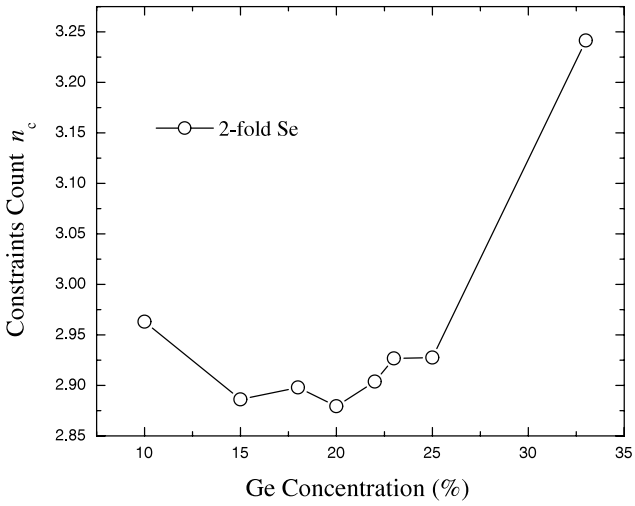

Figure 7. Total constraint count n_c of twofold Se units plotted against Ge concentration x.

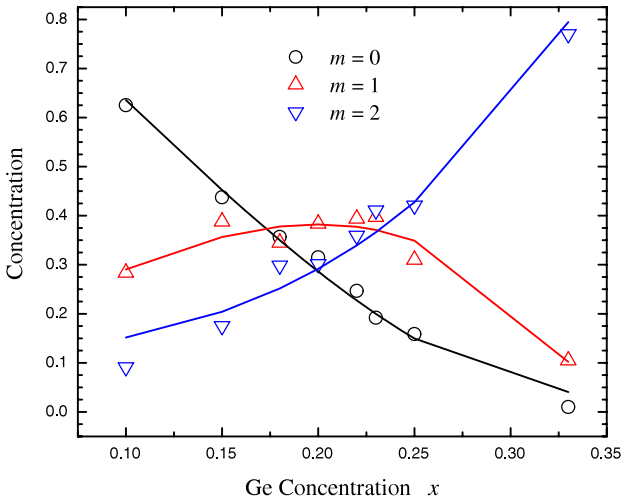

Figure 8. Variation of the concentration of twofold Se $m = 0$, 1 and 2 units fitted with the functions (continuous lines) $a_m + b_m p_m$.

the competition between Se–Se and Se–Ge bonding, and hence we can describe the structural evolution from a-Se_2 to a-$GeSe_2$ as a transition of twofold Se $m = 0$ molecular units to $m = 2$ units, mediated by the appearance of $m = 1$ units with equal numbers of Se–Se and Se–Ge bonds. Probabilities for $m = 0, 1$ and 2 units can be written as $p_0 = (1 - p)^2$, $p_1 = 2p(1 - p)$ and $p_2 = p^2$ respectively [10] (figure 6). Since a real system also contains some undercoordinated and overcoordinated atoms, the actual probabilities for these units can be written as linear functions $a_m + b_m p_m$. Parameters a_m represent the possibilities of formation of these units due to undercoordinated and overcoordinated Se and Ge atoms, and b_m are the Boltzmann factors involved in the formation of these structures as described by Micoulaut *et al* [10].

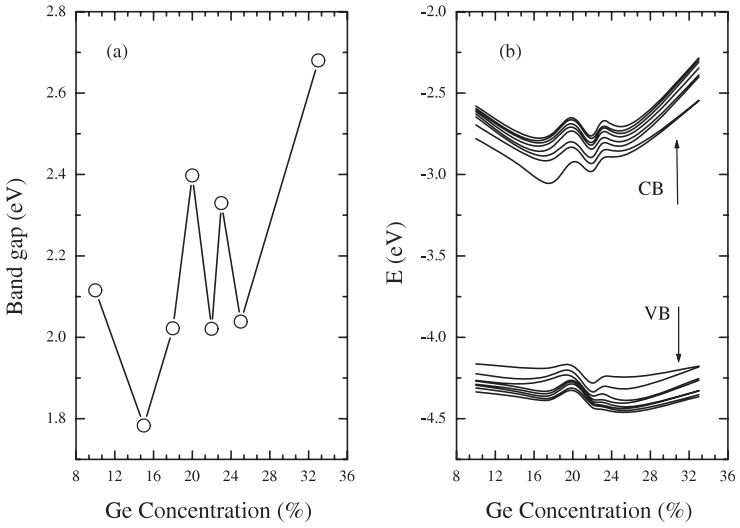

Figure 9. (a) Variation of the estimated optical mobility band gap with the Ge concentration. (b) Fluctuation in the positions of eight localized states at valence and conduction band edges with increasing number of Ge atoms. The large fluctuations from 16 to 27% in (a) are probably artifacts of the statistics of small systems.

Table 1. Fitting parameters a_m and b_m.

	a_m	b_m
$m = 0$	0.04	0.98
$m = 1$	0.08	0.60
$m = 2$	0.12	0.70

We have fitted the concentration variations of these units obtained from our models with these probabilities (figure 8). The fitting shows a nice agreement between the network construction approach developed by Micoulaut *et al* [10] and our models. Fitting parameters are given in table 1. They suggest that the system is approximately minimizing the free energy $F = U - TS$ in the IP window to briefly resist the complete transition from Se–Se bonds to Se–Ge bonds, which results in the 'flattening' of the network evolution (e.g. saturation behavior shown by the mean coordination $\overline{r}$, CST and ring structures (figure 5)) in the IP range of Ge concentration. Self-organization may be viewed as a consequence of this behavior.

6. Electronic properties

We have studied the electronic properties of our models by calculating the electronic density of states (EDOS). Structural characterization of electronic states is done by calculating the inverse participation ratio (IPR), which is given by $\sum_n q(n,i)^2$, where $q(n,i)$ is the Mulliken charge accumulated on atomic site i in an energy state n. Figure 9(a) shows the variation in the mobility band gap with the Ge concentration. We crudely estimate this gap by reporting the splitting between extended states, as we have discussed elsewhere [26]. For small x, the gap is near that of a-Se (2.2 eV [27, 28]). Increase in Ge concentration opens the gap. The trend is similar to what is observed for sputtered thin films of GeSe alloys [29]. Figure 9(b) tracks the behavior of eight states at valence and conduction tail edges. The valence tail states do not

shift appreciably with varying x, while conduction states vary in between $x = 0.18$ and 0.25. It is of interest to observe this behavior in the IP window, apparently representing an electronic signature of the IP. We have computed the projection of the conduction tail states onto various structures in the models and found that 'mixed' bonding (Se atoms bonded to one Ge atom) provides the largest contribution to the states through the IP window, and drops for x outside the IP.

7. Conclusion

In summary we have reported XRD measurements for Ge_xSe_{1-x} alloys, and shown that there is essentially no XRD signature of the IP. First-principles models of these alloys show structural features that might be associated with an intermediate phase. The network evolves from a-Se_2 to $GeSe_2$ through a range of Ge composition which roughly coincides with the IP window, by keeping a relatively high concentration of isostatic twofold Se units having one Se neighbor and one Ge neighbor in this range. This behavior resists the overall structural evolution of the network, probably due to the minimization of the free energy $F = U - TS$ in the IP window. The network evolution in these models in terms of twofold Se units supports the SICA approach developed by Micoulaut *et al* [10]. Increase in the concentration of twofold Se bonded with one Ge in the IP range, isostatic in nature, could be the origin of the lowering of stress in the IP window proposed by Thorpe *et al*. Our work suggests that the IP arises from special local ordering in the IP window in which the network maintains a reasonably constant concentration of the Se_1Ge_1 structures through the IP window as shown in figure 4.

Our work suggests that local experimental probes would be appropriate for exploring our specific predictions about the evolution of local environments in these glasses. Technical details such as the role of quench rates and extensions to other glasses also are under investigation.

Acknowledgments

DAD and FI thank the National Science Foundation for support under grant Nos DMR 0605890, 0600073 and the Army Research Office under MURI W91NF-06-2-0026. MS and SB would like to acknowledge help from Doug Robinson and Billinge group members for help in collecting data. We wish to strongly acknowledge Punit Boolchand for providing the samples. Jim Phillips and Mike Thorpe both made a number of helpful comments on the manuscript. Work in the Billinge group was carried out with the support of the US DOE under contract number DE-FG02-97ER45651. Data were collected at the 6ID-D beam line in the Midwest Universities Collaborative Access Team (MUCAT) sector at the APS. Use of the APS is supported by the US DOE, Office of Science, Office of Basic Energy Sciences, under contract No W-31-109-Eng-38. The MUCAT sector at the APS is supported by the US DOE, Office of Science, Office of Basic Energy Sciences, through the Ames Laboratory under contract No. W-7405-Eng-82.

References

[1] Bychkov E, Benmore C J and Price D L 2005 *Phys. Rev.* B **72** 172107
[2] Bresser W J, Suranyi P and Boolchand P 1986 *Phys. Rev. Lett.* **56** 2493
[3] Boolchand P 1986 *Phys. Rev. Lett.* **57** 3233
[4] Boolchand P, Feng X and Bresser W J 2001 *J. Non-Cryst. Solids* **293–295** 348
[5] Wang F, Mamedov S, Boolchand P, Goodman B and Chandrasekhar M 2005 *Phys. Rev.* B **71** 174201
[6] Boolchand P, Georgiev D G and Goodman B 2001 *J. Optoelectron. Adv. Mater.* **3** 703

[7] Selvanathan D, Bresser W J and Boolchand P 2000 *Phys. Rev.* B **61** 15061
[8] Thorpe M F, Jacobs D J, Chubynsky M V and Phillips J C 2000 *J. Non-Cryst. Solids* **266–269** 859
[9] Micoulaut M 2002 *Europhys. Lett.* **58** 830
[10] Micoulaut M and Phillips J C 2003 *Phys. Rev.* B **67** 104204
[11] Barre J, Bishop A R, Lookman T and Saxena A 2005 *Phys. Rev. Lett.* **94** 208701
Briere M A, Chubynsky M V and Mousseau N 2007 *Phys. Rev.* E **75** 056108
Chubynsky M V, Briére M A and Mousseau N 2006 *Phys. Rev.* E **74** 016116
[12] Sharma D, Samath S, Lalla N P and Awasthi A M 2004 *Physica* B **357** 290
[13] Shatnawi M T, Chen P, Boolchand P and Billinge S J L 2007 submitted
[14] Chupas P J, Qiu X, Hanson J C, Lee P L, Grey C P and Billinge S J L 2003 *J. Appl. Crystallogr.* **36** 1342
[15] Hammersley A P 1998 *ESRF Internal Report* ESRF98HA01T
[16] Qiu X, Thompson J W and Billinge S J L 2004 *J. Appl. Crystallogr.* **37** 678
[17] Demkov A A, Ortega J, Sankey O F and Grumbach M 1995 *Phys. Rev.* B **52** 1618
Sankey O F, Drabold D A and Gibson A 1994 *Phys. Rev.* B **50** 1376
[18] Tafen D and Drabold D A 2005 *Phys. Rev.* B **71** 054206
[19] Cappelletti R L, Cobb M, Drabold D A and Kamitakahara W A 1995 *Phys. Rev.* B **52** 9133
Cobb M, Drabold D A and Cappelletti R L 1996 *Phys. Rev.* B **54** 12162
[20] Zhang X and Drabold D A 2000 *Phys. Rev.* B **62** 15695
[21] Biswas P, Tafen D N, Atta-Fynn R and Drabold D 2004 *J. Phys.: Condens. Matter* **16** S5289
[22] Thorpe M F 1983 *J. Non-Cryst. Solids* **57** 355
[23] Boolchand P and Thorpe M F 1994 *Phys. Rev.* B **50** 10366
[24] Mitkova M and Boolchand P 1998 *J. Non-Cryst. Solids* **240** 1
[25] Micoulaut M, Kerner R and dos Santos-Loff D M 1995 *J. Phys.: Condens. Matter* **7** 8035
[26] Abtew T A and Drabold D A 2007 *Phys. Rev.* B **75** 045201
[27] Mort J 1994 *Phys. Today* **47** 32
[28] Zhang X and Drabold D A 1998 *J. Non-Cryst. Solids* **241** 195
[29] Choi J, Sing A, Davis E A and Gurman S J 1996 *J. Non-Cryst. Solids* **680** 198